ORIGINAL ARTICLE

Variation of three-dimensional femoral bowing and its relation to physical status and bone mineral density: a study with CT

Hiroshi Shimosawa[1] · Takeo Nagura[1] · Kengo Harato[1] · Shu Kobayashi[1] · Masaya Nakamura[1] · Morio Matsumoto[1] · Yasuo Niki[1]

Abstract

Purpose Anatomically, the femoral bone shows sagittal and coronal bowing. Pronounced bowing would affect femoral implant surgery accuracy, but factors associated with degrees of three-dimensional (3D) femoral bowing have not yet been identified. This study measured 3D femoral bowing and examined the correlation between 3D femoral bowing and risk factors.

Methods 3D femoral bone models of unaffected legs from 125 patients were reconstructed from computed tomography data. A trans-epicondylar axis (TEA)-based coordinate system was introduced into bone models and the reproducibility of this coordinate system was evaluated. The cross-sectional contours of the femoral canal were extracted along the vertical axis of the TEA-based coordinate system, and the angles of 3D femoral bowing were examined.

Results The reproducibility to set the coordinate was very high. Total, sagittal, and coronal femoral bowing were $8.9 \pm 1.8°$, $8.7 \pm 1.8°$, and $0.1 \pm 1.9°$, respectively. There was no significant difference in the degrees of femoral bowing between males and females. Total, coronal, and sagittal femoral bowing correlated with age, height, and femoral length, but only femoral coronal bowing correlated with bone mineral density (BMD) of the femur and lumbar spine.

Conclusions We introduced a highly reproducible method for measuring femoral sagittal and coronal bowing by constructing a femoral 3D coordinate system. Anterior femoral bowing was the dominant direction of bowing in our Japanese cohort, whereas the degree of lateral bowing correlated with age, height, femoral length, and BMD. Our results suggest that lateral femoral bowing could increase with aging and decreasing BMD.

Keywords 3D femoral bowing · Computed tomography · Femoral coordinate system · Bone mineral density

Introduction

Anatomically, the femoral bone shows sagittal and coronal bowing [8, 11]. To date, femoral bowing has been analyzed with two-dimensional (2D) radiography by setting the femoral bone axes and measuring the angle between these axes [11, 18, 23]. Reproducibility of the bone axes on 2D radiography is known to have reasonable accuracy and reliability but is influenced by the position of the leg and patients' conditions, such as flexion contracture, valgus/varus deformity, and, especially, lower leg osteoarthritis [2, 14, 19]. To avoid

inaccuracy in the setting of the bone axes, more recently, three-dimensional (3D) computed tomography (CT) has been used to analyze femoral bowing [1, 13, 18]. In these reports, femoral bowing was approximated by a circle and evaluated based on the radius (radius of curvature, ROC). The ROC has been used to evaluate racial differences and side to side differences in femoral bowing [1, 3]. Although the ROC is recognized as a better indicator of femoral bowing than 2D analyses, it is difficult to indicate the degree of femoral bowing with the ROC when the surgeon plans implant surgery into the femur, since surgical planning has traditionally been performed on 2D radiography using the angle of the femoral axis [11, 18, 23]. A method for defining angles in 3D femoral bowing has not yet been established.

For precise analysis, it is important to set 3D coordinates and to determine medial–lateral, anterior–posterior, and proximal–distal directions. A uniform coordinate system is

✉ Takeo Nagura
nagura@z8.keio.jp

1 Department of Orthopaedic Surgery, Keio University School of Medicine, Shinanomachi 35, Shinjyuku-ku, Tokyo 1608582, Japan

the most basic requirement and will promote clear discussion of the bone morphology and development of 3D analyses. For the femur, several coordinates are frequently used [9, 22]. One of them is the trans-epicondylar axis (TEA)-based coordinate system, set with the center of the femoral head and the line between the medial epicondyle and the lateral epicondyle. However, accuracy and reproducibility of setting the TEA coordinate system to 3D femoral bone models have not been evaluated.

It is important to understand variations of femoral bowing in the general population when performing surgery for femoral fracture repair, such as intramedullary rodding to the femur. It has been reported that racial differences in femoral bowing are large; Asian females with knee osteoarthritis have especially pronounced bowing [1, 11]. In an analysis of 3922 femurs of multiple ethnicities, femoral bowing correlated with femur length, but did not correlate with age, body mass index (BMI), or cortical thickness [13]. It was hypothesized that a decrease in BMD could contribute to increased femoral bowing. However, no study has shown an association between femoral bowing and BMD in the general population.

Thus, in the present study, we aimed to evaluate the accuracy and reproducibility of setting the femoral TEA-based coordinate system to 3D bone models, propose a new method to evaluate 3D femoral bowing with CT, and identify subject background factors that correlate with the degree of 3D femoral bowing in the Japanese population.

Materials and methods

This was a cross-sectional study. Institutional review board approval was obtained prior to performing the study, and all patients provided written informed consent prior to enrollment. To evaluate variation in normal femoral bowing, the non-affected side or non-traumatic side was selected for analysis based on the CT images of patients who underwent a CT scan for their diagnosis. We enrolled 38 males (age 12–91, mean 64.0 years) and 87 females (age 27–98, mean 80.3 years), with a total of 125 femoral CT images included in the study. We excluded participants with osteoarthritis (OA), rheumatoid arthritis or osteonecrosis of the lower leg, bilateral femoral bone fracture, or a history of femoral fracture. Primary diagnoses of the patients were as follows (number of cases (number of males:females, mean age)): femoral neck fracture: 40 (9:31, 80.1), femoral trochanteric fracture: 39 (7:32, 83.1), tibial fracture: 10 (6:4, 57.1), ankle fracture: 6 (4:2, 61.3), patella fracture: 4 (1:3, 60), distal femoral fracture: 4 (1:3, 87.3), pelvic fracture: 3 (0:3, 83.3), nonunion after femoral fracture: 2 (1:1, 38), osteochondritis dissecans of the knee: 1 (1:0, 12), talus fracture: 1 (1:0, 76), calcaneal fracture: 1 (0:1,61), anterior cruciate ligament

injury: 2 (2:0, 39), bone bruise of the lower leg: 8 (4:4, 79), and others: 4 (1:3, 61.5). We analyzed the correlation between degrees of femoral bowing and clinical parameters, such as age ($n = 125$), height ($n = 119$), weight ($n = 119$), BMI ($n = 118$), and BMD of the lumbar vertebrae ($n = 112$) and femoral neck ($n = 112$) using dual-energy X-ray absorptiometry. The reason for the disparity in the numbers of participants with missing measurements for height, weight, or BMD was due to the participants' health condition.

Definition of 3D femoral bowing and measurement of femoral length

3D bone models of the femur were reconstructed using 3D imaging software (Mimics, Materialise NV, Leuven, Belgium) based on CT data. Axial CT images of the entire femur, including hip and knee joints, were obtained with 1.0-mm-thick slices (TSX-101A/HA, Toshiba, Japan). The effective radiation dose for CT was below 1 mSv, according to the International Commission on Radiological Protection standards.

We used the TEA-based coordinate system for the evaluation of femoral bowing [22]. To set the coordinate system, three bony landmarks were selected to define the basic planes of the femur. These three bony landmarks were the medial epicondyle, the lateral epicondyle, and the center of the femoral head (Fig. 1). The plane set by these three bony landmarks was defined as the Y–Z plane, the line between the medial epicondyle and the lateral epicondyle (i.e. TEA) was set as the Y-axis, and the point of the lateral epicondyle was selected as the coordinate origin. The XYZ axis was defined with the Y–Z plane (X: anterior/posterior; Y: medial/lateral; Z: proximal/distal). Next, the planes perpendicular to Y–Z planes, with the TEA as the normal vector, and sharing origins were created as X–Z planes. The cross-sectional contours of the femoral canal (cancellous/cortical border) were extracted along the Z axis of the TEA-based coordinate system. Then, the range for cross-sectional slicing was set between the lesser trochanter and the distal end of the epiphysis. For each extracted cross-sectional contour, a least-square fitted ellipse was calculated. Then, a least-square line was fitted to the centers of the cross-sectional ellipses. The proximal anatomical axis was calculated with the proximal half of the ellipse data. Similarly, the distal anatomical axis was determined with the distal half of the data.

The angle between these two axes was measured and defined as total bowing of the femur (Fig. 2). Next, the proximal and distal axes were made to project to these Y–Z planes of the coordinate system, and femoral coronal bowing was examined according to the angles between these projected axes. The directions of lateral bowing were defined as plus directions. Similarly, two axes were made to project to the X–Z planes, and sagittal bowing was examined according to
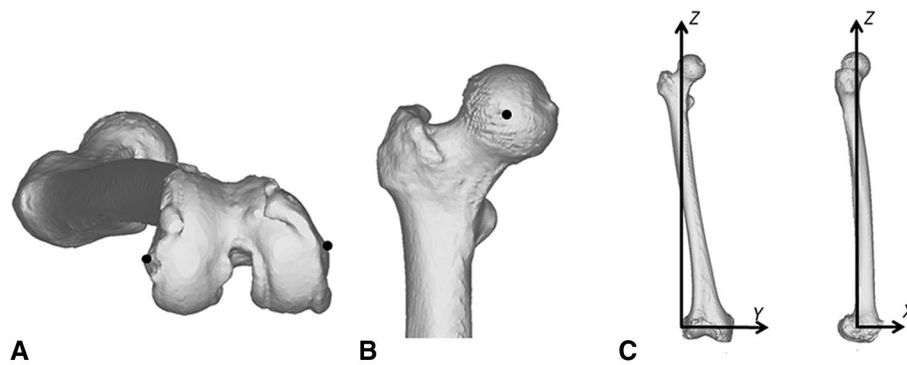
Fig. 1 The TEA (trans-epicondylar axis)-based femoral coordinate system is based on three key bony landmarks including medial and lateral epicondyles of the femur (**a**) and the center of the femoral head (**b**). The plane set by these three bony landmarks was defined as the *Y–Z* plane, the line between the medial epicondyle and the lateral epicondyle (i.e., TEA) was set as the *Y*-axis, and the point of the lateral epicondyle was selected as the coordinate origin. The *XYZ* axis was defined with the *Y–Z* plane (*X*: anterior/posterior; *Y*: medial/lateral; *Z*: proximal/distal). Next, the planes perpendicular to the *Y–Z* planes, regarding the TEA as the normal vector and sharing origins, were created as *X–Z* planes (**c**)
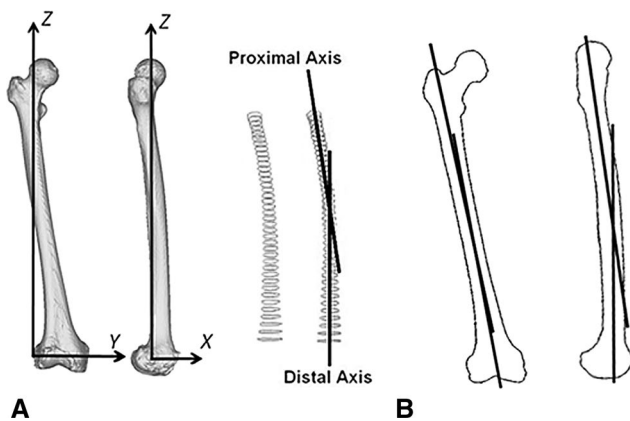
Fig. 2 Definition of the proximal and distal axes (**a**) and measurement of coronal and sagittal bowing in the two different coordinate systems (**b**). The cross-sectional contours of the femoral canal were extracted along the *Z* axis, and the range for the cross-sectional slicing was set between the lesser trochanter and the distal end of the epiphysis. The proximal anatomical axis was calculated with the proximal half of the ellipse data, and the distal anatomical axis was determined with the distal half of the data. Coronal and femoral bowing were measured on the *Y–Z* plane and *X–Z* plane, respectively

the angles between these projected axes (Fig. 2). The directions of anterior bowing were defined as the plus directions. Femoral length was measured as the distance from the most proximal point of the head of the femur to the most distal point of the medial condyle [7].

Evaluation of reproducibility of setting the coordinate system

All observer-dependent steps designating the bony landmarks to establish the TEA-based femoral coordinate system were repeated four times with 20 randomly selected models of femoral bone. The first two observation sets were performed by the first author with an interval of 3 weeks between observations. The third and fourth sets of observations were completed by two other authors. Intra- and interobserver reliabilities were assessed by intraclass correlation coefficients [ICC (1, 1) and ICC (2, 1), respectively].

Statistical analyses

Data for the locations of the bony landmarks are presented as mean ± standard deviation (range), and all statistical analyses were performed using SPSS software (version 18.8; IBM, Armonk, NY). ANOVA was performed using a general linear model to calculate ICC. ICC (1, 1) was calculated from data derived from two measurements performed by one observer; ICC (2, 1) was determined from the average of the measurements of three independent observers. The Shapiro–Wilk test was used to evaluate the distribution of the measured angle for normality; the Levene test was used to assess the homogeneity of variance. For the intra- and interobserver reliabilities, an ICC > 0.7 was considered to represent almost perfect reproducibility [10]. We investigated the correlation between bowing measurements and clinical parameters using Pearson's correlation coefficient.

Results

Reproducibility of three key bony landmarks (the medial and lateral epicondyles and the center of the femoral head) was examined. In terms of ICC, the intra- and interobserver reliabilities were all > 0.99, which implied almost perfect reproducibility (Table 1).

	Intra-Observer Reliability ICC (1,1)	Inter-Observer Reliability ICC (2,1)
Medial epicondyle		
X	1.000	0.999
Y	1.000	0.992
Z	1.000	0.998
Lateral epicondyle		
X	0.999	1.000
Y	1.000	0.997
Z	1.000	0.994
Center of femoral head		
X	0.999	0.999
Y	1.000	0.998
Z	1.000	0.999
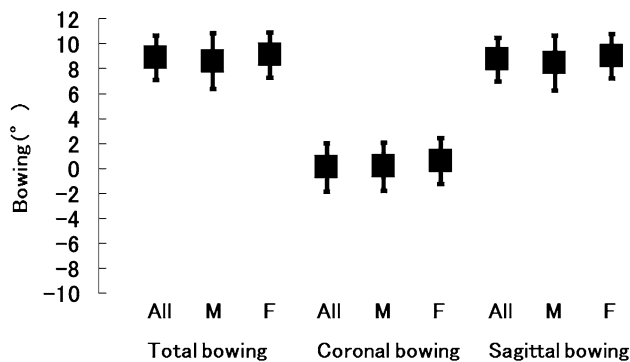
Fig. 3 Sex differences in femoral bowing. There was no statistically significant difference between males and females

Overall, total bowing was $8.9 \pm 1.8°$ (5.1–13.0), sagittal bowing was $8.7 \pm 1.8°$ (4.9–13.1), and coronal bowing was $0.1 \pm 1.9°$ (−4.5–5.3); sagittal bowing was the dominant direction of bowing. There was no statistically significant difference between males and females in terms of 3D femoral

bowing (Fig. 3). To investigate the correlation between background factors and femoral bowing, the correlation coefficients between femoral bowing and the characteristics of all patients are shown in Table 2. Scatter plots of coronal and sagittal bowing with respect to the age, height, lumbar BMD, and femoral neck BMD are presented in Fig. 4. The degree of femoral bowing measurements (total, coronal, and sagittal) positively correlated with age ($p < 0.05$) and negatively correlated with height and femoral length ($p < 0.05$). Lumbar, vertebral, and femoral BMD negatively correlated with coronal bowing ($p < 0.05$).

Discussion

In this study, we clearly defined a method to evaluate 3D femoral bowing angles using CT and showed that anterior femoral bowing was the dominant direction of bowing in our Japanese cohort. Our results are consistent with those of previous reports, and femoral bowing was successfully assessed as an angle with high reproducibility using our method [1, 18].

Limitations in measuring femoral bowing by 2D radiography have been reported [12]. In this report, varus or valgus deformity in the lower limb greatly affected the accuracy in measuring lateral femoral bowing. Other reports also suggest that pain caused by fracture would induce malpositioning on radiography [4, 15]. A method to define 3D lower limb alignment while standing has been reported, and the definition of the femoral axis on 2D radiography was introduced [17]. However, defining the TEA, which is the clinical gold standard for evaluation of femoral morphology and setting the coordinate system of the femur, was not possible with the proposed method. Thus, our method has several advantages over 2D radiography: femoral CT images were not affected by the malpositioning of the patients, coronal and sagittal views were defined with a TEA-based coordinate system, and a clear distinction between sagittal and coronal bowing was possible.

Table 2 Correlation coefficient (p value) between 3D femoral bowing and patient background factors

Parameters	Total bowing	Coronal bowing	Sagittal bowing
Age ($n = 125$)	**0.26 ($p = 0.0039$)**	**0.43 ($p < 0.001$)**	**0.29 ($p = 0.0014$)**
Height ($n = 119$)	**−0.21 ($p = 0.022$)**	**−0.43 ($p < 0.001$)**	**−0.22 ($p = 0.018$)**
Weight ($n = 119$)	−0.11 ($p = 0.22$)	**−0.27 ($p = 0.0033$)**	−0.13 ($p = 0.16$)
BMI ($n = 118$)	0.0061 ($p = 0.95$)	0.035 ($p = 0.70$)	0.029 ($p = 0.75$)
Femur length ($n = 125$)	**−0.19 ($p = 0.030$)**	**−0.36 ($p < 0.01$)**	**−0.20 ($p = 0.026$)**
Lumbar BMD ($n = 112$)	−0.041 ($p = 0.67$)	**−0.36 ($p < 0.001$)**	−0.053 ($p = 0.58$)
Femoral BMD ($n = 112$)	−0.048 ($p = 0.62$)	**−0.37 ($p < 0.001$)**	−0.063 ($p = 0.51$)

The numbers shown in bold indicates statistically significant ($p < 0.05$)

BMI body mass index, *BMD* bone mineral density
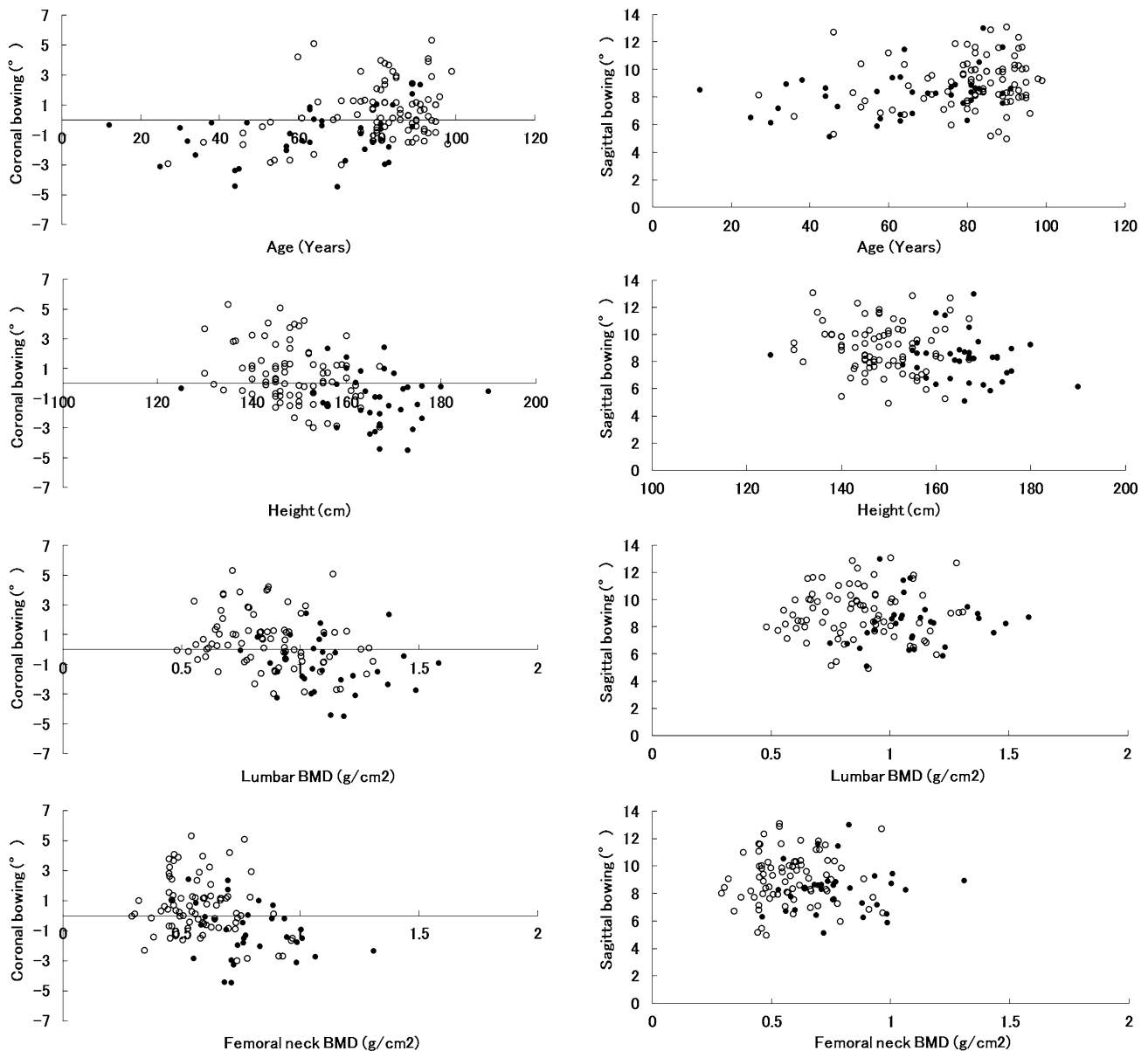
Fig. 4 Scatter plots of the femoral coronal and sagittal bowing compared to age, height, lumbar BMD, and femoral neck BMD for males and females (black = males; white = females). *BMD* bone mineral density

Relatively large variations in femoral bowing among ethnicities have been reported, and a positive correlation between femoral bowing and femoral length has been reported [13]. Another report showed that the Japanese population has greater femoral bowing than other ethnic groups [1]. However, these reports involve younger individuals (average age of 53.5 and 47 years, respectively), and no association between age and femoral bowing was found. In the present study, a positive association between age and femoral bowing (sagittal and coronal) was identified. In addition, a negative correlation between BMD and coronal femoral bowing was noted (Table 2, Fig. 4). This is likely

because our cohort included relatively older aged individuals (average age, 75.3 years), but this is the first report to show a correlation between lateral femoral bowing and BMD. Notably, sagittal bowing did not correlate with BMD. Several previous reports have shown that female patients with knee OA in Asia have especially pronounced lateral bowing in the femur [5, 11, 18]. In addition, the severity of radiological OA was associated with decreased BMD [5]. Moreover, it has been demonstrated that the prevalence of osteoporosis and varus knee OA among Japanese females is higher than that in other industrialized countries [21, 24]. As such, lateral femoral bowing could increase with increased aging and

decreased BMD and could be attributable for varus deformity in the lower limb. To prove this pathogenesis of knee OA, a longitudinal cohort study of the Japanese population is required in the future.

Greater femoral bowing in the Japanese population is an important clinical issue when performing an intramedullary nail procedure on the femur or inserting a stemmed implant in the femur during arthroplasties, since severe bowing of the femur could cause several types of unexpected surgical failures [4, 6, 11, 16, 20, 23]. To avoid such failures, precise analysis of femoral bowing using 3D CT is essential, particularly with aged patients who might have osteoporosis.

The present study has several limitations. The participants enrolled were all patients who had lower leg disease or trauma and femoral bones of the non-affected side were selected, but no healthy controls were included. In addition, there were more female participants and females were of older age compared to male participants. The study design may have increased selection bias.

In conclusion, we successfully introduced a method for measuring femoral sagittal and coronal bowing by constructing a femoral 3D coordinate system with high reproducibility (ICCs of > 0.99). Anterior femoral bowing was the dominant direction of femoral bowing in our Japanese cohort. The degree of lateral femoral bowing correlated with age, height, and BMD, and the results suggest that lateral femoral bowing could increase with aging and decreasing BMD.

Compliance with ethical standards

References

1. Abdelaal AH, Yamamoto N, Hayashi K, Takeuchi A, Morsy AF, Miwa S, Kajino Y, Rubio DA, Tsuchiya H (2016) Radiological assessment of the femoral bowing in Japanese population. SICOT J 22:2–7
2. Chang CB, Choi JY, Koh IJ, Seo ES, Seong SC, Kim TK (2010) What should be considered in using standard knee radiographs to estimate mechanical alignment of the knee? Osteoarthr Cartil 18:530–538
3. Dimitriou D, Tsai TY, Yue B, Rubash HE, Kwon YM, Li G (2016) Side-to-side variation in normal femoral morphology: 3D CT analysis of 122 femurs. Orthop Traumatol Surg Res 102:91–97
4. Egol KA, Chang EY, Cvitkovic J, Kummer FJ, Koval KJ (2004) Mismatch of current intramedullary nails with the anterior bow of the femur. J Orthop Trauma 18:410–415
5. Im GI, Kwon OJ, Kim CH (2014) The relationship between osteoarthritis of the knee and bone mineral density of proximal femur: a cross-sectional study from a Korean population in women. Clin Orthop Surg 6:420–425
6. Jiang CC, Insall JN (1989) Effect of rotation on the axial alignment of the femur. Pitfalls in the use of femoral intramedullary guides in total knee arthroplasty. Clin Orthop Relat Res 248:50–56
7. Khanal L, Shah S, Koirala S (2017) Estimation of total length of femur from its proximal and distal segmental measurements of disarticulated femur bones of Nepalese population using regression equation Method. J Clin Diagn Res 11(3):1–5
8. Karakaş HM, Harma A (2008) Femoral shaft bowing with age: a digital radiological study of Anatolian Caucasian adults. Diagn Interv Radiol 14:29–32
9. Kingsley PC, Olmsted KL (1948) A study to determine the angle of anteversion of the neck of the femur. J Bone Joint Surg Am 30A:745–751
10. Landis JR, Koch GG (1977) The measurement of observer agreement for categorical data. Biometrics 33:159–174
11. Lasam MP, Lee KJ, Chang CB, Kang YG, Kim TK (2013) Femoral lateral bowing and varus condylar orientation are prevalent and affect axial alignment of TKA in Koreans. Clin Orthop Relat Res 471:1472–1483
12. Li YR, Gao YH, Qi X, Liu JG, Ding L, Yang C, Zhang Z, Li SQ (2017) Analysis of factors that affect the precision of the radiographic lateral femoral bowing angle using a three-dimensional computed tomography-based modelling technique. J Orthop Surg Res 14(12):92
13. Maratt J, Schilling PL, Holcombe S, Dougherty R, Murphy R, Wang SC, Goulet JA (2014) Variation in the femoral bow: a novel high-throughput analysis of 3922 femurs on cross-sectional imaging. J Orthop Trauma 28:6–9
14. Matsumoto T, Hashimura M, Takayama K, Ishida K, Kawakami Y, Matsuzaki T, Nakano N, Matsushita T, Kuroda R, Kurosaka M (2015) A radiographic analysis of alignment of the lower extremities—initiation and progression of varus-type knee osteoarthritis. Osteoarthr Cartil 23:217–223
15. Mochizuki T, Tanifuji O, Koga Y, Sato T, Kobayashi K, Nishino K, Watanabe S, Ariumi A, Fujii T, Yamagiwa H, Omori G, Endo N (2017) Sex differences in femoral deformity determined using three-dimensional assessment for osteoarthritic knees. Knee Surg Sports Traumatol Arthrosc 25:468–476
16. Park JH, Lee Y, Shon OJ, Shon HC, Kim JW (2016) Surgical tips of intramedullary nailing in severely bowed femurs in atypical femur fractures: simulation with 3D printed model. Injury 47:1318–1324
17. Sato T, Koga Y, Omori G (2004) Three-dimensional lower extremity alignment assessment system: application to evaluation of component position after total knee arthroplasty. J Arthroplasty 19:620–628
18. Sebastian AS, Wilke BK, Taunton MJ, Trousdale RT (2014) Femoral bow predicts postoperative malalignment in revision total knee arthroplasty. J Arthroplasty 29:1605–1609
19. Skyttä ET, Haapamäki V, Koivikko M, Huhtala H, Remes V (2011) Reliability of the hip-to-ankle radiograph in determining the knee and implant alignment after total knee arthroplasty. Acta Orthop Belg 77:329–335
20. Tetreault MW, Shukla SK, Yi PH, Sporer SM, Della Valle CJ (2014) Are short fully coated stems adequate for "simple" femoral revisions? Clin Orthop Relat Res 472:577–583
21. Wade SW, Strader C, Fitzpatrick LA, Anthony MS, O'Malley CD (2014) Estimating prevalence of osteoporosis: examples from industrialized countries. Arch Osteoporos 9:182

22. Wu G, van der Helm FC, Veeger HE, Makhsous M, Van Roy P, Anglin C, Nagels J, Karduna AR, McQuade K, Wang X, Werner FW, Buchholz B (2002) Standardization and Terminology Committee of the International Society of Biomechanics. ISB recommendation on definitions of joint coordinate system of various joints for the reporting of human joint motion—part I: ankle, hip, and spine. International Society of Biomechanics. J Biomech 35:543–548

23. Yau WP, Chiu KY, Tang WM, Ng TP (2007) Coronal bowing of the femur and tibia in Chinese: its incidence and effects on total knee arthroplasty planning. J Orthop Surg (Hong Kong) 15:32–36

24. Yoshimura N, Muraki S, Oka H, Mabuchi A, En-Yo Y, Yoshida M, Saika A, Yoshida H, Suzuki T, Yamamoto S, Ishibashi H, Kawaguchi H, Nakamura K, Akune T (2009) Prevalence of knee osteoarthritis, lumbar spondylosis, and osteoporosis in Japanese men and women: the research on osteoarthritis/osteoporosis against disability study. J Bone Miner Metab 27:620–628